**NATIONAL UNIVERSITY OF
SCIENCE AND TECHNOLOGY
POLITEHNICA OF BUCHAREST**

**Doctoral School of Electronics, Telecommunications
and Information Technology**

Decision No. 84 **from** 19-07-2024

Ph.D. THESIS
SUMMARY

Eng. George-Stelian MUSCALU

MICROSISTEME DE CAPTARE A ENERGIEI PENTRU APLICAȚII DE MEDIU

ENERGY HARVESTING MICROSYSTEMS FOR ENVIRONMENTAL APPLICATIONS

THESIS COMMITTEE

Prof. Dr. Ing. Ion MARGHESCU
National University of Science and Technology Politehnica of Bucharest — President

Prof. Dr. Ing. Gheorghe BREZEANU
National University of Science and Technology Politehnica of Bucharest — PhD Supervisor

Prof. Dr. Ing. Radu VASIU
Politehnica University of Timisoara — Referee

CS I. Dr. Ing. Carmen-Aura MOLDOVAN
NIRD for Microtehnologies IMT-București — Referee

Dr. Ing. Adrian TULBURE
National University of Science and Technology Politehnica of Bucharest — Referee

BUCHAREST 2024

Content

Chapter 1

Introduction

1.1 Presentation of the field of the doctoral thesis

In an increasingly connected society, the sensors represent an important part in the advancing of the informational world. The main trends in their development are: portability, miniaturization, advanced techniques of integration, connectivity, security and reliability. Thus, in addressing these trends, there have been increasing requirements for low-energy consumption and, therefore, ultra-low power integrated circuits have been developed, from a few µW up to hundreds of µW [1].

Energy harvesting **is the process of extracting a low quantity of energy from the ambient environment**. In other words, by energy harvesting, the available energy from the ambient environment is transformed in electrical energy. This thesis focusses on the energy from the mechanical vibrations, a type of energy which could be harvested by piezoelectricity.

The piezoelectric energy harvesting microsystems are fabricated using MEMS technologies and represent a good solution for generating small quantities of energy from the ambient vibrations. This demand for safe systems which should be energy efficient, reliable and minimum-to-none maintenance led to an increasing market for energy harvesters, a market which could reach $0.9 billion up to 2028 [2].

The piezoelectric energy harvesting microsystems, or piezoelectric energy harvesters, could offer a **high efficiency for energy conversion** and a **good compatibility for miniaturization**. Their purpose is to collect mechanical energy, in this case, the one from ambient vibrations, and transform it in electrical energy by **the direct piezoelectric effect** (inducing a stress in the piezoelectric material).

1.2 Scope of the doctoral thesis

The present work proposes the development of **new piezoelectric energy harvesters**, fabricated by **MEMS technology** for industrial, automotive, aerospace or civil infrastructure applications.

The **purpose** of the project is the developing of **new energy harvesting technologies from the ambient environment** for the autonomous operation of **ultra-low-power** microsensors, wireless sensor nodes or portable systems, **in the range of 1-100µW.** The mechanism of energy generation/harvesting is presented in **Fig. 1.1**.
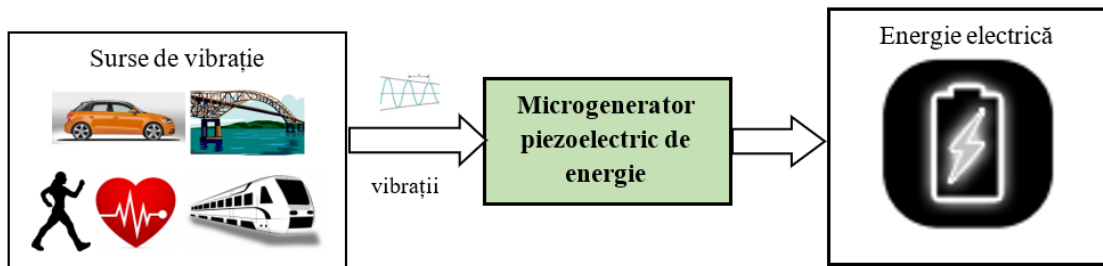
Fig. 1.1 The mechanism for the energy harvesting

Different piezoelectric materials were considered: lead-free materials, as zinc oxide (ZnO), doped zinc oxide, aluminum nitrate (AlN), doped aluminum nitrate or potassium-sodium-niobate (KNN) and lead-based materials as well, as lead-zirconate-titanate (PZT).

1.3 Content of the doctoral thesis

The present work contains 6 chapters that analyze the design, simulation and fabrication steps for some MEMS-technologies-based piezoelectric energy harvesters for industrial and automotive applications. Also, additional to these 6 chapters, the thesis includes 3 annexes in which the process for testing piezoelectric materials is described, as well as less successful manufacturing attempts of piezoelectric energy harvesters for aerospace and civil infrastructure applications.

Chapter 1 presents the field of the doctoral thesis by a short introduction for the need of energy harvesters and a summary of a few mechanical vibration's sources. These led to the outline of the purpose of the work.

Chapter 2 shows a summary for the state-of-the-art of piezoelectric energy harvesters manufacturing. This summary was a key-element in achieving a theoretical background for the harvester's fabrication.

Different cantilever structures were designed and simulated in **chapter 3**. The focus of these structures was two types of applications, industrial and automotive, and led to two types of energy harvesting microsystems, PZU1 and PZU2.

Chapter 4 describes the fabrication technologies for the two types of energy harvesters.

The testing for the fabricated MEMS structures is presented in **chapter 5**. The testing was done in laboratory conditions, for both types of harvesters, and in relevant conditions as well, for the automotive applications harvester.

Chapter 6 summarize the general conclusions and presents the obtained results. The author's original results are highlighted separately, in correlation with the published scientific papers during the PhD period. The perspectives for further developments are presented in the last section, perspectives that cover both independent technological processes and the energy harvester as a system.

Annex 1 presents the testing structures for piezoelectric materials and the less successful manufacturing attempts of other piezoelectric energy harvesters are shown in **annexes 2 and 3**. These harvesters were for aerospace and civil infrastructure applications. Even though these results were modest, they were an important learning step for the fabrication of the PZU2 energy harvester.

Chapter 2

Piezoelectric energy harvesters – theoretical considerations

2.1 State-of-the-art – selection

The main energy sources from ambient environment are: solar, wind, acoustic, thermoelectrical and mechanical vibrations. The focus of the project is on the mechanical vibrations.

The project's purpose is the developing of a MEMS microgenerator using silicon technology for harvesting energy from mechanical vibrations and converse it to electrical energy. All the studied harvesters were based on the **mechanical structure of a cantilever** as a resonator structure which vibrates on its own resonant frequency. In this case, the cantilever means a silicon beam fixed on one of its ends with or without a proof mass at the tip.

In 2014, Jackson et al. evaluate three piezoelectric MEMS energy harvesters for low accelerations. The same piezoelectric material was used for all three (AlN). Power density of 24-100µW/cm^3 were obtained for accelerations of 0.2-0.4g and resonant frequency of 97-149Hz [3]. Also, they obtained an increase in the frequency bandwidth from which the harvest took place by using a cantilever array.

A version of a energy harvester with a wide beam cantilever was also presented by Jia et al. in 2016 [4]. A power of 20.47µW was obtained at a resonant frequency of 210Hz and an acceleration of 0.27g.

Silicon-based micromachining technologies were employed for the fabrication of the energy harvesters.

2.2 Micromachining technologies

Understanding of the silicon-based micromachining technologies is crucial in developing and fabrication of the energy harvesters. These technologies could be classified in two main categories: **bulk micromachining** and **surface micromachining**.

The **thermal oxidation (thermal growth)** is used to grow high quality amorphous silicon oxide on silicon wafers.

The **Chemical Vapor Deposition (CVD)** is based on the thermal decomposition and/or reaction of gaseous compounds and the desired material deposition on the substrate surface, directly from the material's gaseous state.

The **Physical Vapor Deposition (PVD)** is used for obtaining thin layers of material (from few nm to few µm). The PVD processes are vacuum deposition techniques with a low impact upon the environment. The most used PVD techniques are **evaporation** and **sputtering**.

Lithography is a technological process in which patterns are formed in a chemical-resistant polymer (resist/photoresist) which in turn was applied on a silicon wafer. After the exposure of the polymer to a type of radiation, the polymer's composition is modified, it becomes soluble or insoluble (depending on its type) and it could be removed resulting in its patterning.

The **etching** consists in selective removing of a material. A patterned photoresist is commonly used as an etching mask. The etching could be wet or dry etching.

The **wet etching** is a chemical process which is isotropic in amorphous materials (like SiO_2) and it could be anisotropic in crystalline materials (Si). The chemical etching consists in the next steps: chemical reactants movement at the surface, chemical reactive etching and the removing of reaction products.

Dry etching or plasma etching implies the generating of chemical reagents, neutrals (F, Cl) and ions (SF_x^+), which are accelerated by an electric field to a target substrate. Isotropic dry etching takes place in a plasma of sulfur hexafluoride (SF_6) and is used as an alternative to wet etching. **The Bosch process** is the most used process for the anisotropic dry etching of silicon. This process uses alternative steps of passivation and etching. Passivation takes place by deposition of a polymer with the function of protecting the lateral walls. The etching process will mainly remove the material at the bottom of the geometry.

The **stop-etching mechanisms** are essential in the etching processes. These are: etch-stopping by areas which were heavily-doped with boron, electrochemical etch-stopping, etch-stopping by reaction time and etch-stopping by buried oxide layers.

2.3 Piezoelectrical energy harvester

The piezoelectricity is the material's property of changing its polarization state (to accumulate electric charge) under the influence of a mechanical force (direct piezoelectric effect) and to mechanically distort under the influence of an electric voltage (reverse piezoelectric effect).

The piezoelectric materials have a preset polarization and they respond differently to stress, depending on the direction of the elastic wave. There are two main **electromechanical coupling modes**: **transversal mode** (d31 – the direction of the elastic wave is perpendicular to the direction of the electric field) and **longitudinal mode** (d33 – the elastic wave and the electric field have the same direction).

The purpose of the design is to collect mechanical energy from a vibrational source and to obtain a power as high as possible. For this, **the harvester should resonate on the same resonant frequency with the targeted vibrational source**. For a rectangular cantilever structure, the following equation could be used for the **resonant frequency** [5]:

$$f = \frac{1}{2\pi}\sqrt{\frac{k}{m}} = \frac{1}{2\pi}\sqrt{\frac{Y_{eq}Wt^3}{4L^3(m_i + 0.24m_c)}} \tag{2.13}$$

where Y_{eq} is the equivalent of the Young's modulus of cantilever, W, t and L are the width, thickness and length of the cantilever, m_i and m_c are the inertial and the cantilever mass.

The **output power** is dependable of the **thickness** and the **electromechanical coupling modes** of the piezoelectric material, and the cantilever's **morphology** as well.

Chapter 3

Design and simulation of the piezoelectric energy harvesters

3.1 Schematic diagram. Design data

The piezoelectric energy harvester is designed as a cantilever structure. Silicon micromachining technologies and the parameters described in chapter 2 were taken into consideration for the harvester's design. The schematic diagram from **Fig. 3.1** played an important role in the design. This presents two types of piezoelectric energy harvesters, based on the mechanical structure of a cantilever: one with planar electrodes, designed to work in the transversal coupling mode (**Fig. 3.1a**), and one with inter-digited electrodes, designed to work in the longitudinal coupling mode (**Fig. 3.1b**). The inertial mass (m.i.), or proof mass, has the role to reduce the resonant frequency of the cantilever.

(a)

(b)
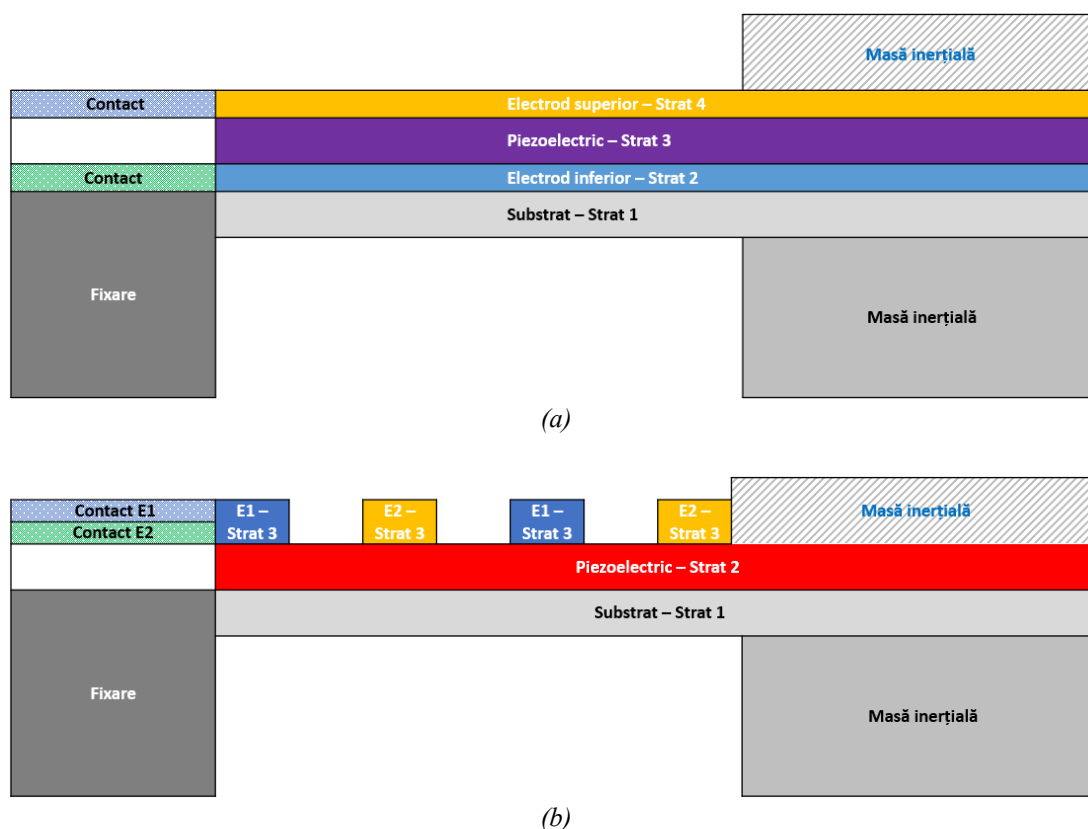
Fig. 3.1 *Schematic diagram of a piezoelectric energy harvester: (a) with planar electrodes for the d31 coupling mode; (b) with inter-digited electrodes for the d33 coupling mode*

3.2 Piezoelectric energy harvester for industrial applications – PZU1

For the industrial field, a possible application could be the monitoring of different equipment from a production line or from factories for an optimized maintenance.

This type of energy harvester was developed during my first research project. Some limitations were imposed, as the chip area (1 cm^2), the new proposed design (an array with 2x10 cantilevers) and lead-free materials. With these considerations and with resonant frequencies of hundreds of Hz for industrial equipment, a range of 400-500 Hz was chosen for the desired energy harvester.

The design and simulation for the energy harvester were also presented in previous papers, for example in [6]. The design was made according with the structure described in **Fig. 3.1a** and with the design data from **Table 3.1**.

Table 3.1 *Design data of the energy harvester for industrial applications*

Chip area	1 cm^2	Cantilever length	2500μm
Design/Geometry	a 2x10 cantilevers array	Cantilever width	300μm
Morphology	Uni-morph	Cantilever thickness	10μm
Materials	Lead-free	Inertial mass (m.i.)	YES
Young's modulus	Material properties	Length m.i.	1200μm
Density	Material properties	Width m. i.	300μm
Resonant frequency	400-500 Hz	Thickness m.i.	400μm
Coupling mode	Transversal (d31)		

FEM-based *(Finite Element Method)* simulations were runed first, using COMSOL Multiphysics software. The initial resonant frequency was 448Hz, but, after an optimization for the technological process (described in chapter 4.2), the cantilever structure was redesigned and its new resonant frequency was 435Hz (**Fig. 3.8**), which was still in the desired range of 400-500Hz. **Fig. 3.11** shows the concept for the PZU1 harvester, with an array of 20 cantilevers.
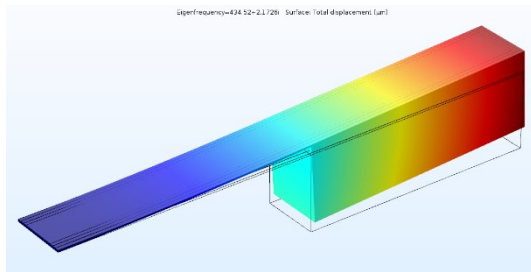
Fig. 3.8. *The resonant frequency of the redesigned structure, 435Hz*
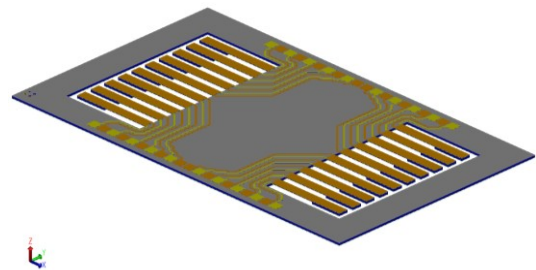
Fig. 3.11. *Energy harvester concept, with an array of 2x10 cantilevers*

3.3 Piezoelectric energy harvester for automotive applications – PZU2

All the previous experience, which was acquired in designing the energy harvesters described in **chapters 3.2, 4.2, 5.2 and Annexes 2 and 3**, was a major input in designing the PZU2 energy harvester.

The targeted resonant frequency was chosen using vibrations' measurements, provided by Renault Technologie Roumanie (RTR) at Titu Technical Centre. The measurements were made on a Dacia Jogger car, as in the example from **Fig. 3.12**. The measurements led to a desired frequencies spectrum, as in **Fig. 3.13**.
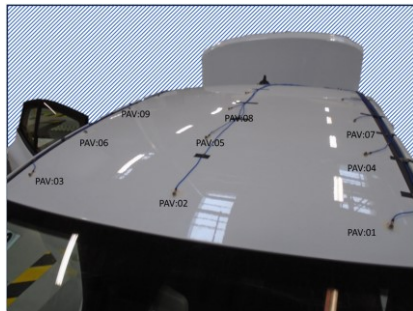
Fig. 3.12 *Example of a vibration's measurements setup on a car*
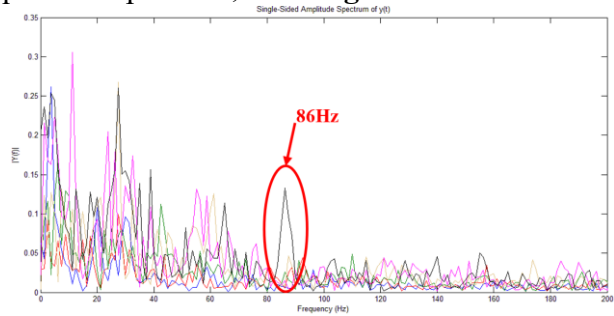
Fig. 3.13 *The resulted frequencies spectrum from the vibrations' measurements*

The designed resonant frequency was chosen according with the technological capabilities from IMT-Bucharest and the desired application from RTR. The back part of the car was taken into consideration as a possible placement of the energy harvester. A motivation could be the increased cost in placing voltage-supplied wires at the back of the car, as well as providing maintenance. Therefore, the 86Hz frequency was targeted for this harvester. The design data are presented in **Table 3.4**. PZT was chosen as the piezoelectric material because of its better piezoelectric coefficients between the available materials. Also, PZT allows us in using the longitudinal coupling mode (**Fig. 3.1b**), which could provide an easier fabrication process. Based on the simulations, the first vibration mode was at 87Hz (**Fig. 3.16**).

Table 3.4 *Design data of the energy harvester for automotive applications*

Chip area	$1\ cm^2$	Cantilever length	$8800\ \mu m$
Design/Geometry	1 wide cantilever	Cantilever width	$7450\ \mu m$
Morphology	Uni-morph	Cantilever thickness	$20\ \mu m$
Materials	PZT	Inertial mass (m.i.)	YES
Young's modulus	Material properties	Length m.i.	$4400 \mu m$
Density	Material properties	Width m. i.	$7450 \mu m$
Resonant frequency	86 Hz	Thickness m.i.	$510 \mu m$
Coupling mode	Longitudinal (d33)		
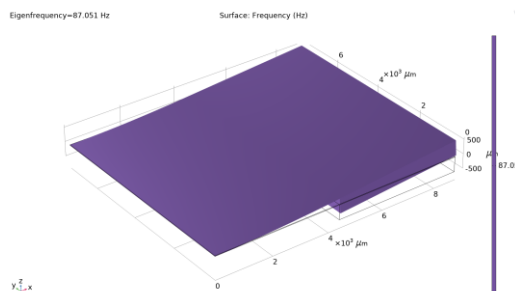
Fig. 3.16. *First vibration mode, 87Hz*

Chapter 4

Fabrication technologies for the energy harvesters

4.1 Initial considerations

In this chapter, the designs of the fabrication technologies for the energy harvesters were developed. These consist in the design and fabrication of technological masks and choosing the best technological processes for the energy harvesters' development.

In designing and fabricating the technological masks and choosing the best technological processes, some aspects were taken into consideration, such as: the need of releasing the chips in a non-destructive manner, bulk micromachining of silicon, stop-etching techniques, chips' handling, the piezoelectric properties and how are influenced by the technological processes.

4.2 Piezoelectric energy harvester for industrial applications – PZU1

Starting from the schematic diagram from **Fig. 3.1a** and the concept from **Fig. 3.11**, the technological masks and process flow were developed. Various techniques for the bulk micromachining of silicon were used in the device fabrication. A few examples are: anisotropic dry etching, front-back alignment or stop-etching techniques.

The SOI wafers (*Silicon on Insulator*) are needed in the process flow. These are described by their 3 component layers: a device layer, a buried-oxide layer with the role of insulator and the handler layer as a mechanical support (mainly). In this case, the buried oxide layer has also a role in stopping the silicon etching, thus resulting a better control for the final etching process.

Initially, the process flow for the fabrication of the PZU1 harvesters consisted in using 5 technological masks (**Fig. 4.1**) and 3" SOI wafers. The SOI wafers had a thickness for the device layer of 10μm, 0.5μm for the buried oxide and 400μm for the handler. The masks were designed with a distance of 200μm between the cantilevers. The whole process flow was designed in using the positive photo-resist.

The process flow starts with a thermal growth of silicon oxide of 0.5μm, which has the role of an insulator. The bottom electrode (Ti-Pt, 20nm-200nm) is deposited and patterned over this oxide layer using Mask 1 (**Fig 4.1a**) and the lift-off technique. Then, the piezoelectric layer (1μm) is deposited and patterned using Mask 2 (**Fig. 4.1b**) and the top electrode (Cr-Au, 20nm-200nm) results using Mask 3 (**Fig. 4.1c**).

a)

b)

c)

d)

e)
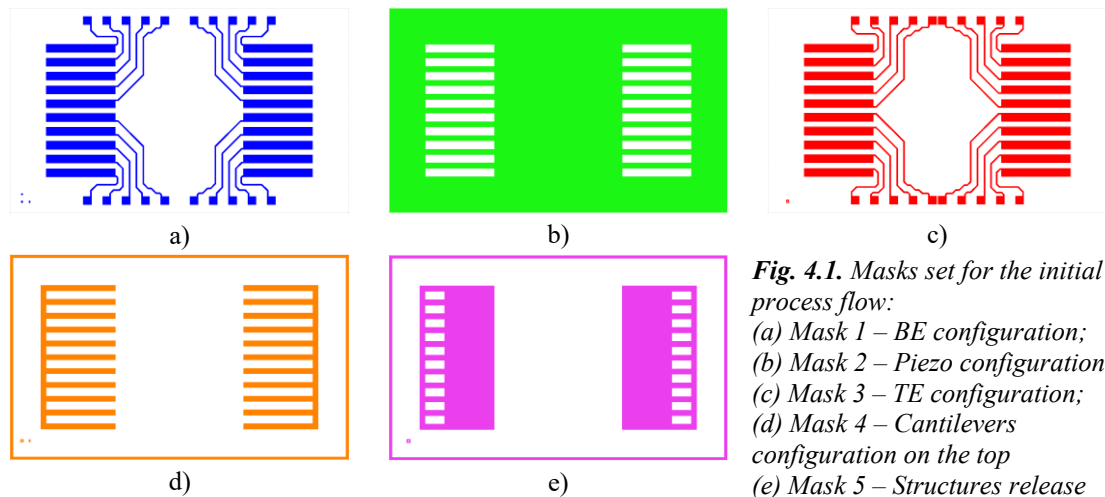
Fig. 4.1. Masks set for the initial process flow:
(a) Mask 1 – BE configuration;
(b) Mask 2 – Piezo configuration;
(c) Mask 3 – TE configuration;
(d) Mask 4 – Cantilevers configuration on the top
(e) Mask 5 – Structures release

The back of the wafer is protected by a photo-resist deposition and its front is processed using Mask 4 (**Fig. 4.1d**). This process has the role of configuring the cantilevers using a wet etching for SiO_2 and a dry etching for the 10μm of silicon. The dry etching consists in a DRIE etching (*Deep Reactive Ion Etching*), using the Bosch process. The buried oxide is used as a stop-etching layer in this case.

After that, the front of the wafer is protected by photo-resist and the processing takes place on its back, using Mask 5 (**Fig. 4.1e**). Again, SiO_2 is etched using wet etching and silicon is etched using DRIE (about 400μm).

Some **technological challenges** appeared during the initial processing of the energy harvesters: difficulties in the integration of the piezoelectric materials with MEMS technologies, obtaining suitable metallic layers for the piezoelectric materials deposition and the release of the cantilever structures.

The integration of piezoelectric materials with MEMS technologies was studied using the test structures described in **Annex 1**. Several piezoelectric materials were studied, as zinc oxide (ZnO), doped zinc oxide, KNN, aluminum nitrate (AlN) or doped aluminum nitrate.

The manganese- and vanadium-doped zinc oxide layers were deposited using the sol-gel technique but the results were incompatible with the available MEMS technology. The layers were either too thin and irregular (as in the case of Mn-doped ZnO, **Fig. 4.2a**) or strongly irregular (as in the case of V-doped ZnO, **Fig. 4.3a**).

The usage of a ZnO layer deposited by sputtering led to redesigning the masks in order to avoid a short-circuit between the planar electrodes. The short-circuit was caused by an over-etch of the ZnO (**Fig. 4.4b**). In the end, this ZnO layer did not had the desired piezoelectrical properties but its compatibility with MEMS technologies led to a validation of the process flow at IMT-Bucharest.
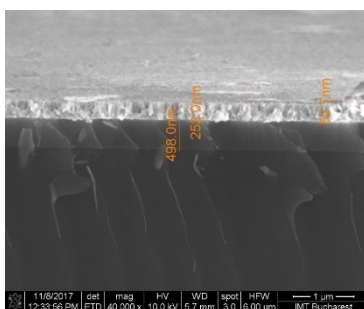
Fig. 4.2a. Mn-doped ZnO samples – SEM image
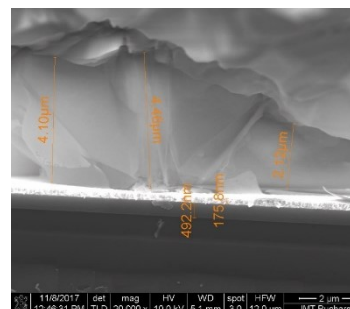
Fig. 4.3a. V-doped ZnO samples – SEM image
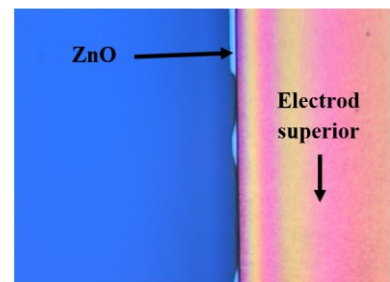
Fig. 4.4b. Over-etching of ZnO and short-circuit between electrodes

The KNN piezoelectric layers were deposited on platinum layers due to their need of high-temperature treatment, about 700°C. These had a weak adhesion to the substrate but this challenge led to a study regarding the improvement of platinum layers deposited at IMT-Bucharest [7]. The study consists in different thermal treatments of the deposited platinum layers by varying the temperature, 450-700°C, the atmosphere, like inert gas (argon), air or forming gas (H_2:N_2 1:6). The studied parameters were the crystallography of the platinum layers and their sheet resistance. The experiments led to an improvement in the crystallography of platinum on the (111) direction for air and forming gas treatments at 500°C. The air treatment is better because it offers a decrease of the unwanted peaks (**Fig. 4.12**). The sheet resistance decreases with the temperature for all the studied treatments but the lowest value is achieved using air (**Table 4.2**). The results from this study also led in improving other types of sensors, like gas sensors or biomedical sensors.
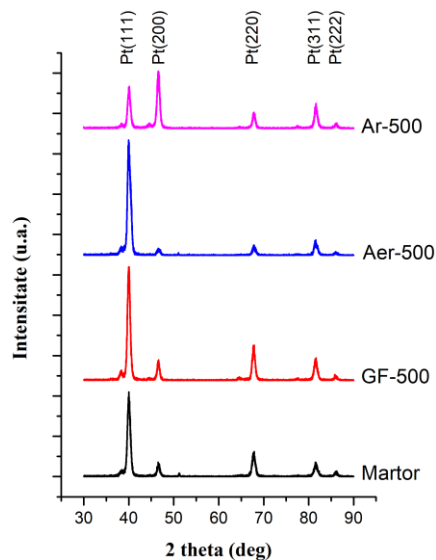
Fig. 4.12 GIXRD characterization for the as-deposited sample and Pt/Ti samples treated in argon (500°C), air (500°C), forming gas (500°C), 30 de minute

Table 4.2. Sheet resistance vs temperature for the studied treatments.

Temp. [°C]	R_s [mΩ/□]		
	Ar	**Air**	**Forming gas**
450	797	658.5	715
500	711.5	602	718.5
550	664.5	602	578
600	622.5	590	585
650	629	550.5	546.5
700	597	514.5	566

The technological challenges regarding the release of the cantilever structures were overcome by successive designs for the processing masks. Thus, starting from a process in which the cantilevers were still trapped in silicon (**Fig. 4.18**), by redesigning the masks fully-released structures were obtained (**Fig. 4.26**). The final masks set also implies a redesign of the electrodes in order to avoid short-circuits (**Fig. 4.4b**), increasing the distance between cantilevers from 200µm to 300µm and including sacrificial structures on Mask 5 (**Fig. 4.27e**) in order to level the etching rate of the DRIE process across the wafer. The final set is shown in **Fig. 4.27** and the fabricated devices are shown in **Fig. 28-29**.
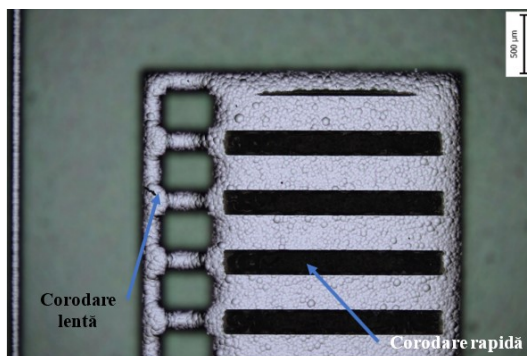
Fig. 4.18 Microscope imagine: DRIE etching on the back of the wafer with the initial masks

Fig. 4.26. Fully-released structures on silicon standard wafers

a)

b)

c)

Fig. 4.27. *Final masks set for the PZU1 harvester:*
(a) Mask 1 – BE configuration;
(b) Mask 2 – Piezo configuration;
(c) Mask 3 – TE configuration;
(d) Mask 4 – Cantilevers configuration on the top
(e) Mask 5 – Structures release

d)

e)
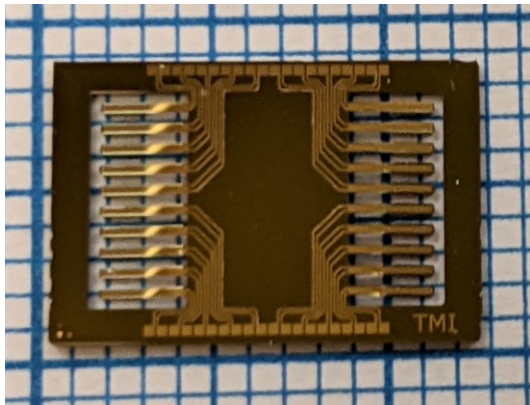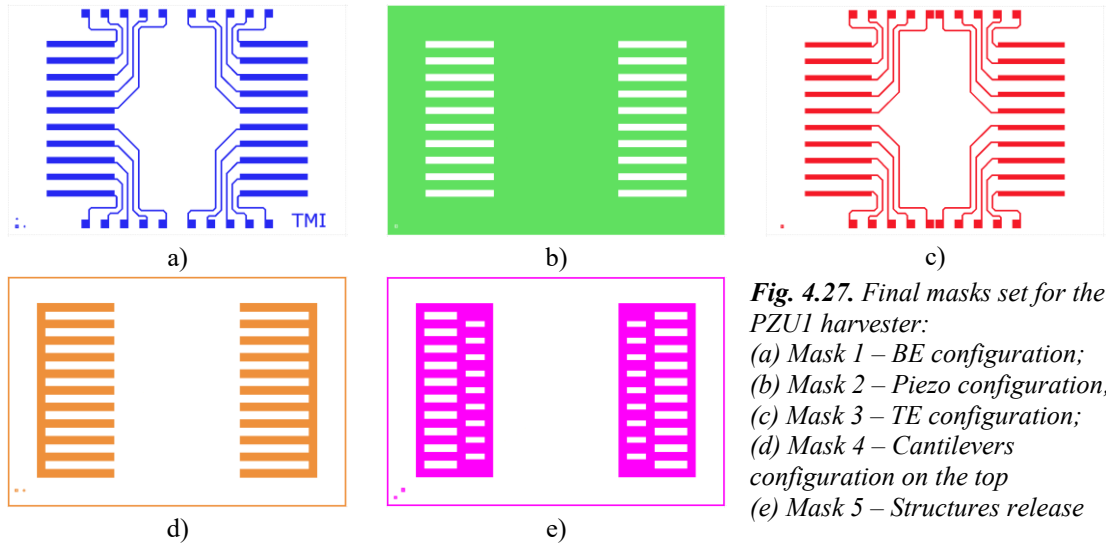
Fig. 4.28. *Fabricated PZU1 energy harvester*
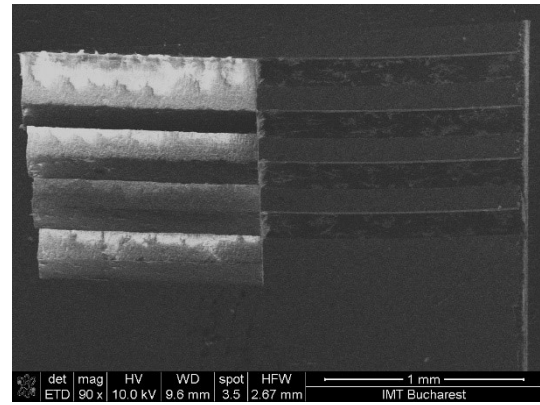
Fig. 4.29. *SEM detail for an array of cantilevers from the PZU1 energy harvester*

4.3 Piezoelectric energy harvester for automotive applications – PZU2

All the previous experience was taken into consideration in designing the process flow for the PZU2 energy harvester. This experience was described in **chapter 4.2** but also in **Annexes 2 and 3** and it made anything to go more smoothly and faster.

The PZU2 energy harvester design takes into consideration the schematic from **Fig. 3.1b** and its process masks are presented in **Fig. 4.30**. The piezoelectric material is PZT, a material with very good piezoelectric coefficients on the longitudinal coupling mode as well. This coupling mode implies the usage of inter-digited electrodes (IDE) and the process flow could be much easier.

The process flow starts with SOI wafers (device layer of 20μm, buried oxide of 1μm and handler layer of 510μm), on which, a silicon oxide layer of 0.5μm is thermally grown for insulating purposes. A seed layer is deposited over this silicon oxide in order to facilitate the deposition of the piezoelectric material and to improve the insulation of the oxide. The piezoelectric material is also deposited and, over it, the inter-digited electrodes (IDE – Cr-Au 20nm-200nm) are deposited and patterned

using Mask 1 (**Fig. 4.30a**). After this, on the front of the wafer, several etchings are following using Mask 2 (**Fig. 4.30b**) in order to pattern the PZT material, the seed layer, thermally grown silicon oxide and the 20µm of silicon. The front of the wafer is protected using parylene and the process continues on the back of the wafer using Mask 3 (**Fig. 4.30c**), for structures release.

| (a) | (b) | (c) |
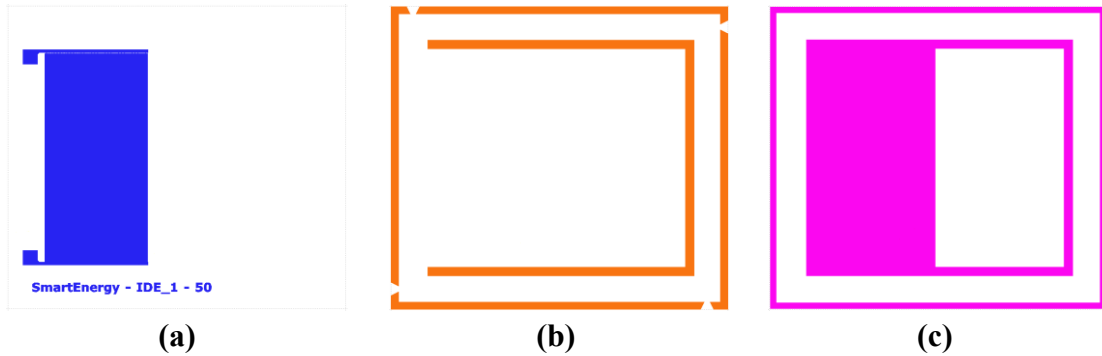
Fig. 4.30. *Masks set for the fabrication of PZU2 energy harvester:*
(a) ***Mask 1*** *– IDE configuration; (b)* ***Mask 2*** *– Cantilever conf.; (c)* ***Mask 3*** *– Structure release;*

The fabricated PZU2 energy harvester is shown in **Fig. 4.31**. The IDE electrodes were designed in order for the polling process of the piezoelectric material to be done in its whole thickness. Polling the piezoelectric material means applying a direct voltage at a specific temperature for a certain amount of time. After polling, the PZT crystallography is changed and better piezoelectric coefficients are obtained. For an optimum polling process of a **PZT layer of 1.1µm**, the **IDE were designed with a width of 4µm and a spacing of 6µm**. The IDE electrodes cover only the base of the cantilever, on an area of 3540 µm × 7130µm. Here, the stress in the piezoelectric material exhibits a maximum value. In the polling process the direct voltage varied between 30V and 80V, for 15 minutes at a temperature of 150°C (on a hot plate). The best results were for the 80V treatment (**Fig. 4.35**).
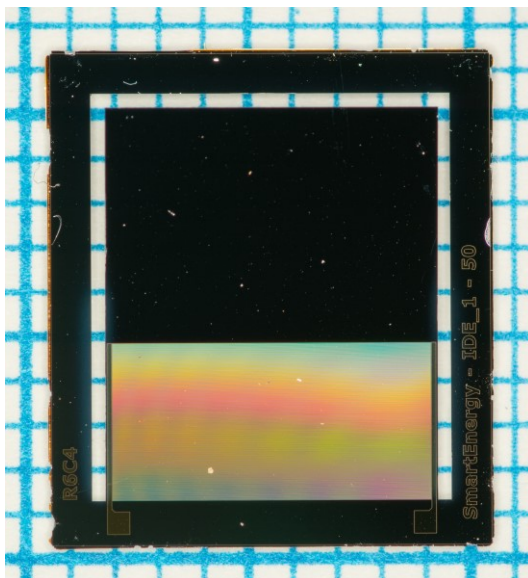
Fig. 4.31. *The fabricated PZU2 energy harvester*
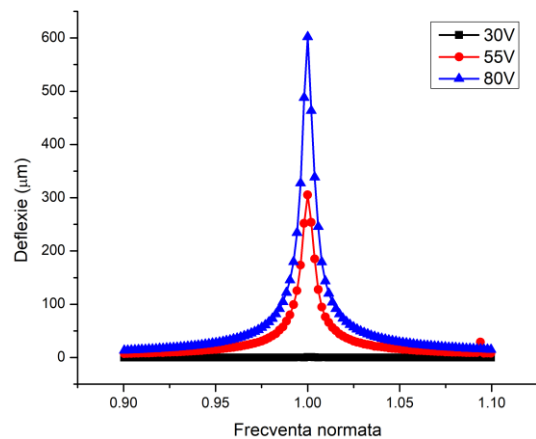
Fig. 4.35. *The harvester's response at different polling voltages, around the resonant frequency: 30V, 55V, 80V*

Chapter 5

Testing of the energy harvesters

5.1 Experimental setup and the electronic module

Two experimental setups were created for testing of the two energy harvesters, one for each of the harvesters. Both setups consist in a function generator, an amplifier, a vibrations exciter on which the device under test (DUT) is placed, together with an accelerometer for monitoring the vibrations. The signals of interest are measured on an oscilloscope (probe 10MΩ, 8pF). An initial version for one of these setups is shown in **Fig. 5.2**. This one was used in testing the PZU1 energy harvesters and it is using an audio amplifier and a speaker as a vibration's exciter. These components could faithfully reproduce the desired vibrations, in the range of 400-500Hz. The experimental setup shown in **Fig. 5.3** was used for testing the PZU2 energy harvesters. The amplifier and the exciter are designed for these types of tests and they allow testing on a much larger frequencies bandwidth, including low frequencies of 80-100Hz.
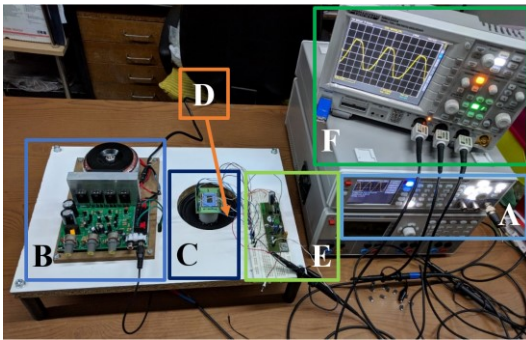
Fig. 5.2. Experimental setup for testing energy harvesters for industrial applications:
A – function generator; B – amplifier;
C – exciter; D – DUT with accelerometer;
E – electronic module; F – oscilloscope
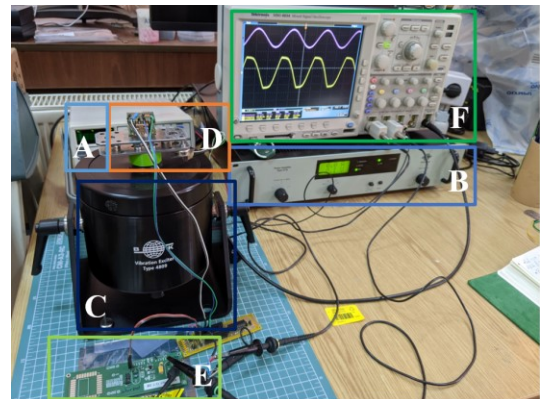
Fig. 5.3. Experimental setup for testing energy harvesters for automotive applications:
A – function generator; B – amplifier;
C – exciter; D – DUT with accelerometer;
E – electronic module; F – oscilloscope

The purpose of the energy harvesters is to be used in supplying energy to sensors or microsystems. In this regard, it is necessary in using an electronic module in order to obtain a stabilized voltage. A commercial solution was chosen in developing the electronic module, by using the LTC3588-1 integrated circuit. This integrates a low-loss full-bridge rectifier and a Buck converter, optimized for ultra-low power applications.

Two versions were considered for the electronic module: version A, which offers the possibility of choosing the desired stabilized voltage between 1.8V, 2.5V, 3.3V or 3.6V, and version B, a compact version which could only provide 1.8V. Version A

was chosen in the end (**Fig. 5.4**). The energy harvester (PZ_eq) is connected to PZ1 and PZ2 pins, which are the inputs pins for the full-bridge rectifier. The harvested energy is rectified and stored on the input capacitor C_{in}. When the voltage on this capacitor reaches a threshold voltage of 4.06V, the stored energy is transferred, through the Buch converter, on the output capacitor, C_{out}. The cycle is repeated until the output voltage, V_{out}, reaches the chosen stabilized voltage. This condition is reached when the P_{good} signal has the logical value of "1".
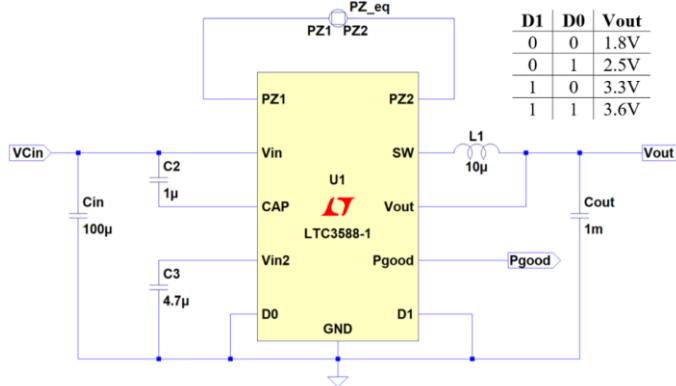
Fig. 5.4. *Stabilized and stored circuit for the energy harvester – version A*

5.2 Energy harvester testing for industrial applications – PZU1

Given the design for the PZU1 energy harvester (an array with 2x10 cantilevers), a key step in its developing were the measurements of cantilevers' vibration at ITE-Poland, using a Doppler interferometer, MSA-500 de la Polytec (Irvine, CA, USA) – **Fig. 5.9**. Following these measurements, we obtained the resonant frequency, the quality factor and phase for each cantilever.

The measurements were possible by using a ceramic packaging, developed by HIPOT-RR (Otocec, Slovenia), and fixing it on a PCB for easy access to the cantilever pads (**Fig. 5.10**). The cantilevers were grouped in quadrants and the results are given in **Table 5.1**, which was fully reproduced from our own paper [8].

Table 5.1. *Measurements results using a Doppler interferometer*

Quadrant	Cantilever														
	1			2			3			4			5		
	f [Hz]	Q	φ [°]	f [Hz]	Q	φ [°]	f [Hz]	Q	φ [°]	f [Hz]	Q	φ [°]	f [Hz]	Q	φ [°]
1	465.4	1751	-	465.3	2028	19.34	464.8	1909	32.47	465.3	1854	19.21	456.2	1824	23.12
2	462.2	1383	19.33	464.6	1423	23.01	468.3	2397	21.56	468	1357	27.7	463.4	2069	32.46
3	462.3	1782	21.48	475.2	930	N/A	482.2	820	44.1	463.6	1865	72.48	463.7	1735	N/A
4	464.2	N/A	-4.8	476.1	1915	18.41	464.1	1600	20.89	464	1634	19.51	461.7	1790	N/A
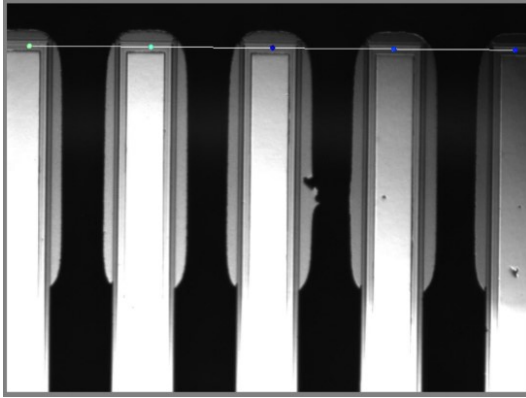
Fig. 5.9. Resonant frequencies measurements using a Doppler interferometer
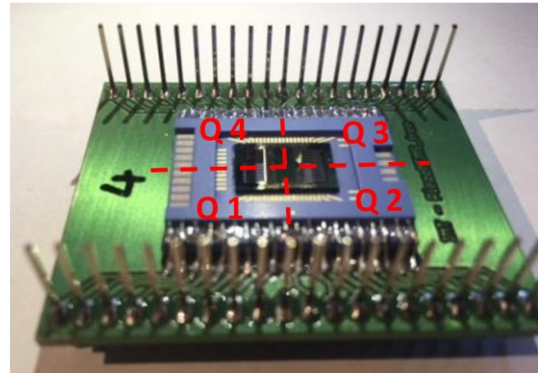
Fig. 5.10. Cantilevers grouping in quadrants

A first observation is that the resulted frequencies are in the desired range, of 400-500Hz. The variation of frequencies is in a 26Hz bandwidth. The high-quality factor makes for this variation to be significant. Also, a difference between the cantilevers' phases could also be observed. This further influences the electrical performance of the energy harvester.

The difference between the cantilevers' phases prevents the connection of all the 20 cantilevers in a way of improving the electrical output of the energy harvester. A possible solution is in grouping only some cantilevers, with similar phases. In this regard, 10 cantilevers were chosen from **Table 5.1**. Their phases were between 18 and 23°. Ways of connecting the 10 cantilevers were elaborated in the own paper, presented at CAS 2018 conference [9]. The conclusion was to connect the 10 cantilevers in 2 branches in series, with 5 cantilevers connected in parallel on each branch (*5p2s* group).

The advantage of connecting multiple cantilevers is shown in **Fig. 5.14.** The generated signal by the 5p2s group is significantly larger than any signal from a single cantilever. The measurements were made at an acceleration of 1g. Also, the 5p2s group harvests energy from a larger bandwidth than a single cantilever.

Starting this point, only the 5p2s group gets analyzed, at its **resonant frequency of 465.2Hz**. In **Fig. 5.15,** the generated signal of the group is shown, as a peak-to-peak voltage, when the acceleration is increasing. There is a rapidly growing signal at 0.8g and 1.7g. A possible explanation could be a better coupling between the 10 cantilevers. During experiments, there was slight variation of the resonant frequency (de +/- 1Hz) by increasing the acceleration.

Fig. 5.16 and 5.17 present the harvester response to the load resistance variation and the generated electrical power. The load resistance axis is presented in logarithmic scale.

At a resonant frequency of 465.2Hz and an acceleration of 1g, **the maximum electric power was of 2.53μW** for an **optimum load resistance of 1MΩ**. The resulted **power density** is **60.2nW/mm^3**.
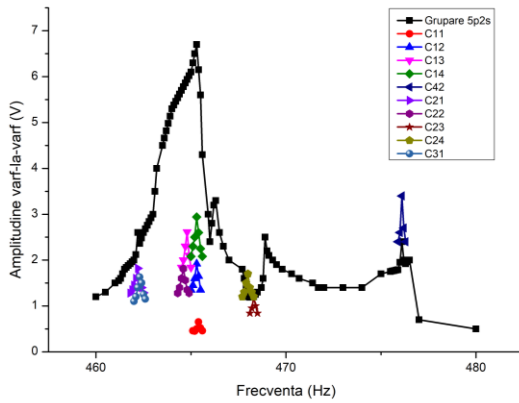
Fig. 5.14. *5p2s group in relation with its component cantilevers – acceleration of 1g*
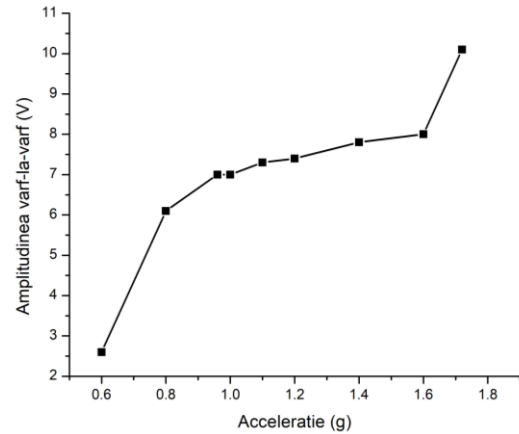
Fig. 5.15. *Peak-to-peak amplitude of 5p2s group to acceleration variation*
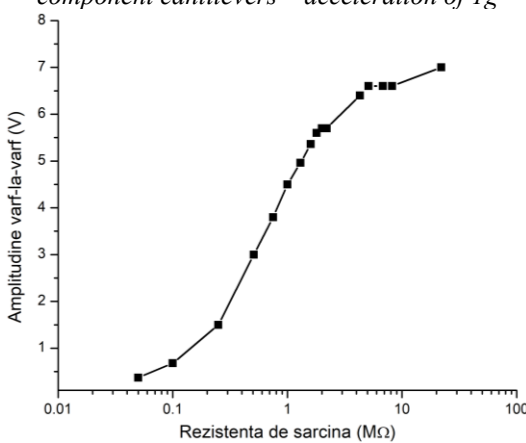
Fig. 5.16. *Peak-to-peak amplitude of 5p2s group to load resistance variation*
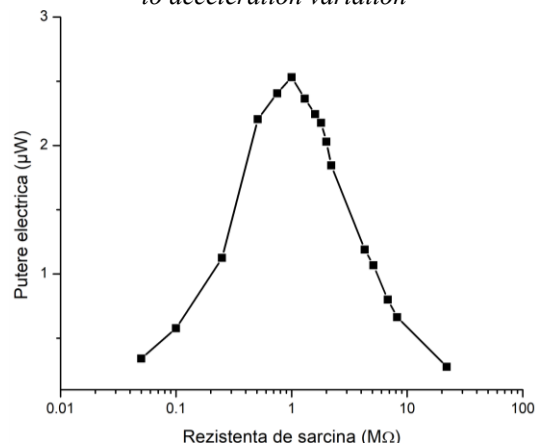
Fig. 5.17. *Electrical power of 5p2s group to acceleration variation*

For an **acceleration of around 2g**, the energy harvester together with the electronic module could provide a **stabilized voltage of 1.8V** (**Fig. 5.21**), measured at the V_{out} pin in the electrical circuit from **Fig. 5.4**. Larger values for the capacitors mean a longer time for charging and stabilizing but could provide a longer connection to the load (up to a few seconds).
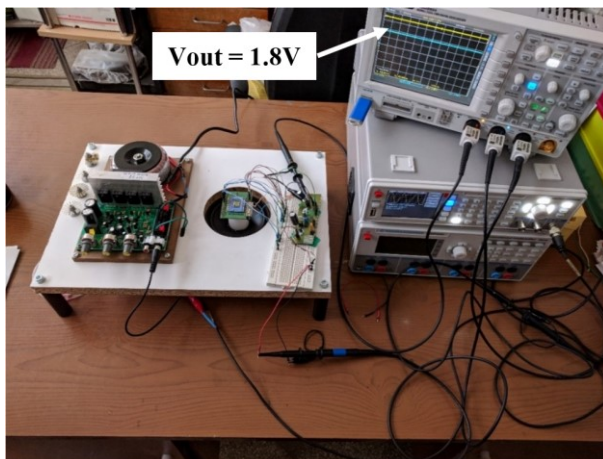
Fig. 5.21. *LTC3588-1 functionality together with the PZU1 energy harvester;*
On oscilloscope: Vout = 1.8V (experimental setup)

The results presented in this section were published in the paper "Piezoelectric MEMS Energy Harvester for Low-Power Applications", Electronics 2024, 13(11), 2087; https://doi.org/10.3390/electronics13112087 [8].

5.3 Piezoelectric energy harvester for automotive applications – PZU2

In this case, the PZU2 energy harvester was mounted on a specially designed PCB (*Printed Circuit Board*), without a ceramic packaging – **Fig. 5.23**. One or two harvesters could be mounted on this PCB. Connecting a second harvester could bring a voltage or a current gain. These harvesters were tested in the experimental setup from **Fig. 5.3**.

Because the used case for this harvester was represented by the automotive applications, its testing was done at a lower acceleration,
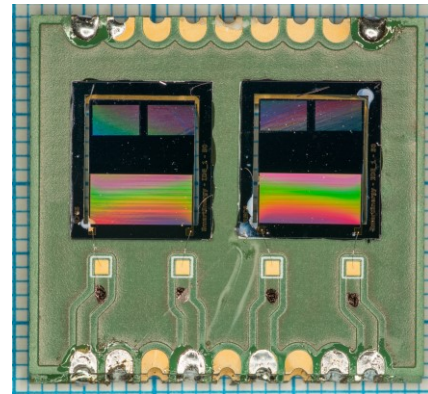
Fig. 5.23. PZU2 energy harvester, mounted on PCB

between 0.2g and 0.6g. A single harvester was tested at a time, without connecting it to others.

The dependence of the peak-to-peak voltage around the resonant frequency is shown in **Fig. 5.25**, for an acceleration of 0.2g. The resulted resonant frequency was around 86Hz, accordingly to the desired specifications.

The relation of the peak-to-peak amplitude to acceleration variation is presented in **Fig. 5.26.** In comparison with the harvester from section 5.2, the PZU2 variation has a linear dependence, being only one wide cantilever.
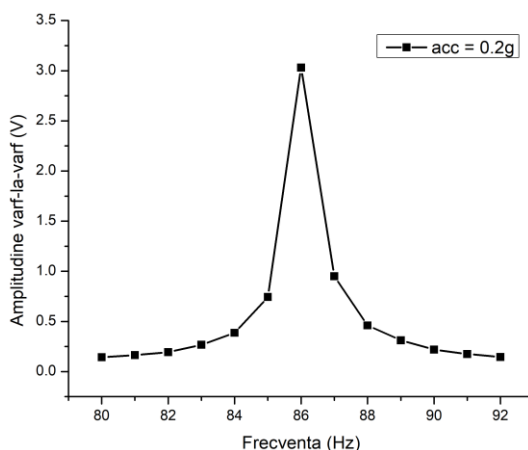
Fig. 5.25. Peak-to-peak amplitude arount the resonant frequency
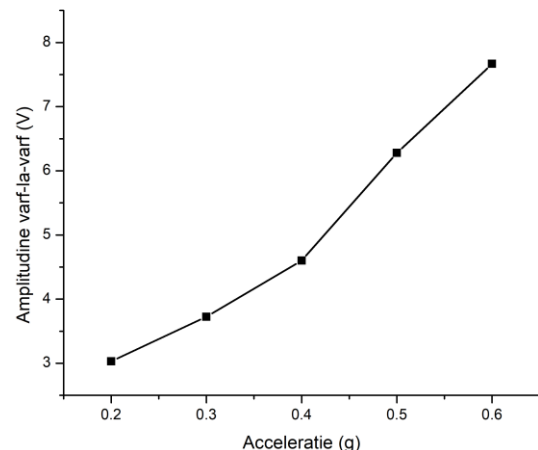
Fig. 5.26. Peak-to-peak amplitude to the acceleration variation

Fig 5.27 shows the peak-to-peak amplitude to the load resistance variation and the resulted electrical power is shown in **Fig. 5.28**. The testing accelerations were of low value, similar to the one on the driving car. The X axis is represented on a logarithmic scale.

At a resonant frequency of 86Hz and an acceleration of 0.4g, the **maximum electrical power is 2.28μW** for an **optimum load resistance of 250kΩ**. The resulted **power density is 69.5nW/mm^3**.
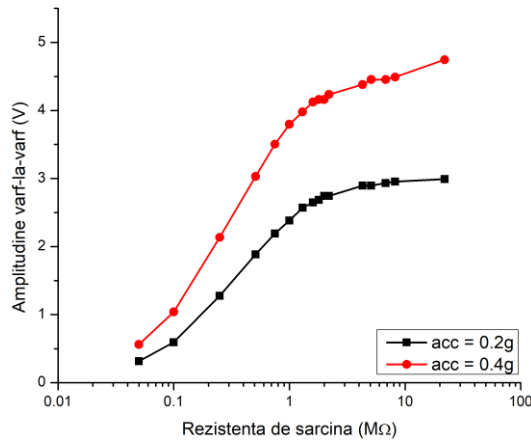
Fig. 5.27. *Peak-to-peak amplitude to load resistance variation*
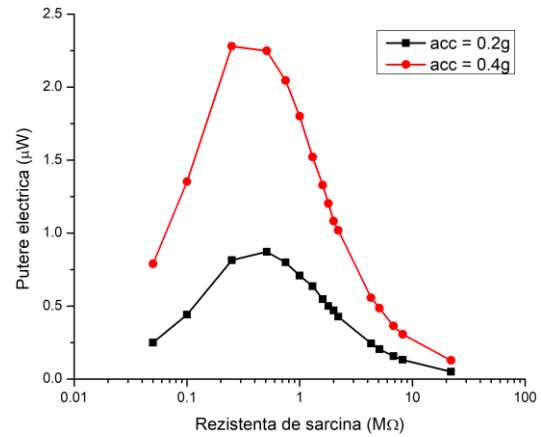
Fig. 5.28. *Electrical power to load resistance variation*

A stabilized voltage was also obtained in this case, but in special laboratory conditions. For this, 5 PZU2 energy harvesters were connected in parallel and the acceleration was gradually increased, up to 2.5g. A stabilized voltage of 2.5V was obtained using the electrical schematic from **Fig. 5.4** and replacing the output capacitor with a supercapacitor. The supercapacitor was encapsulated in a CR2032 or CR2016 package and it was provided by Swistor SA (Laussane, Elveția). The stabilization was obtained in around 12 minutes of continuous excitation (**Fig 5.30**).
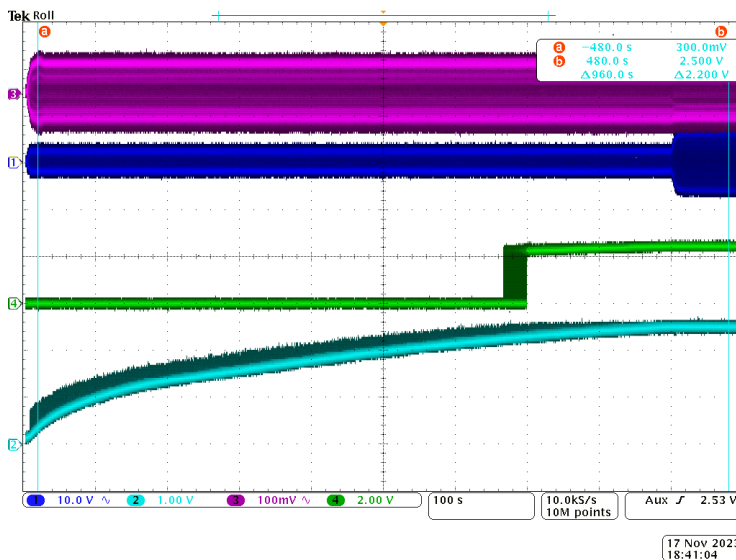
Fig. 5.30. *A stabilized voltage of 2.5V, for special laboratory conditions:*
1. magenta – accelerometer
2. blue – 5× PZU2 in parallel
3. green – PGOOD signal
4. cyan – supercapacitor voltage/ output voltage

In this case, the PZU2 energy harvester testing was also possible in relevant conditions, on a Dacia Jogger car at the Titu Technical Centre, Renault Technologie Roumanie (Bucharest, Romania).

3 scenarios were tested: **scenario 1** (starting from the spot and up to 50km/h and 70km/h speeds), **scenario 2** (starting from the spot and up to 70km/h and 120km/h) and **scenario 3** (starting from the spot, speed up to 50km/h, stop and repeat the cycle up to 3 times).

Two types of harvesters were tested in similar conditions: the fabricated PZU2 energy harvesters and some commercial ones (MIDE PPA 1021) from Mide Technolgy (Woburn, MA, USA). The resonant frequency for the commercial ones was set to 86Hz. The results are shown in **Table 5.2.**

From a power density point of view, the results were similar between the two types of harvesters. The best results were for the 2nd scenario (**Fig. 5.32**), where a power density of 46.10nW/mm^3 was obtained. The measured accelerations were below 0.5g. In **Fig. 5.34,** the two types of harvesters are shown, as a comparison between their dimensions.

These results were disseminated at EpoSS Annual Forum conference [10].

Tabel 5.2. *Relevant conditions measurements for the PZU2 energy harvester*

Scenario	Microgenerator	Resonant frequency (Hz)	Dimension (L × W × t mm^3)	Electrical power (μW)	Power density (nW/mm^3)
1	MIDE PPA 1021	86	54 × 10.3 × 8.1	104.63	23.22
	PZU2	86	8.8 × 7.45 × 0.5	0.67	20.39
2	MIDE PPA 1021	86	54 × 10.3 × 8.1	225.16	49.98
	PZU2	86	8.8 × 7.45 × 0.5	1.51	46.10
3	MIDE PPA 1021	86	54 × 10.3 × 8.1	97.91	21.73
	PZU2	86	8.8 × 7.45 × 0.5	0.66	20.12
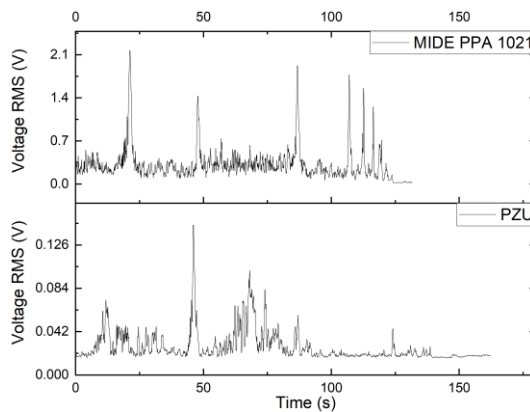
Fig. 5.32. Relevant conditions measurements – Scenario 2
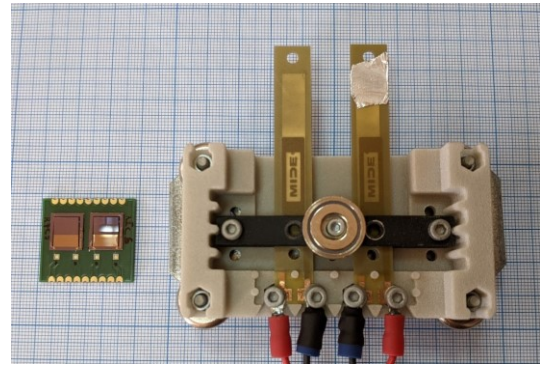
Fig. 5.34. Comparison between the two harvesters, PZU2 (left) and MIDE PPA 1021 (right)

5.4 Comparison with similar energy harvesters

In order to level the differences between different energy harvesters, the power density is normalized to the square of acceleration. For this, only the resonator volume was taken into consideration (together with the spacings between cantilevers for certain cases). The results are shown in **Table 5.3**, a partially reproduced table from paper [8]. The results are similar between the selected references.

Table 5.3. *Comparison with similar energy harvesters - selection*

Microgenerator	Material	Dimensions (mm^3)	Resonant freq. (Hz)	Acceleration (g)	Power$_{max}$ (μW)	Power density (μW· mm^{-3}·g^{-2})
PZU1	ScAlN	2 × (2.5 × 5.7 × 0.412)	465.3	1	2.53	0.215
PZU2	PZT	8.8 × 7.45 × 0.5	86	0.4	2.28	0.434
Liu et al. [11]	ScAlN/AlN	4.02 × 4 × 0.551	1357.5	1	1.7	0.192
He et al. [12]	AlN	13 × 14 × 0.402	160.6	1	54.1	0.74
Zhao et al. [13]	AlN	11 × 12.12 × 0.502	230.4	1	3.249	0.048
Jackson et al. Narrow [3]	AlN	7.5 × 1 × 0.562	97	0.4	0.38	0.56

Chapter 6

Conclusions

This thesis approached possible applications for the piezoelectric energy harvesters by designing and simulating several types of these microsystems using the FEM-based (FEM – Finite Element Method) techniques.

Therefore, two solutions were designed, fabricated and tested, for two different types of applications: industrial and automotive. The harvesters for industrial applications were only tested at a laboratory level but relevant-conditions tests were also possible for the ones for automotive applications.

The piezoelectric energy harvesters could be a viable solution as an alternative supply source, in certain conditions. These conditions are defined by the existing vibrations in the ambient environment for a certain application. These vibrations are characterized by their magnitude (acceleration) and their resonant frequencies.

6.1 Obtained results

All the presented results meant a step forward in achieving the final goal, which was the one to develop microsystems capable to harvest energy from the environment in order to offer a supply voltage for sensors or other ultra-low power microsystems for the industrial and automotive applications.

Chapter 1 defines the field of the thesis using a short introduction for the need of the energy harvesters, which in turn led to outline the purpose and motivation for this research.

Chapter 2 presents the state-of-the-art for piezoelectric energy harvesters' fabrication and the theoretical considerations for their design and fabrication. The theoretical considerations consist in silicon micromachining technologies, in the mechanical structure for a cantilever and the material properties for piezoelectric materials.

Chapter 3 is dedicated to designing and simulating of the energy harvesters. The design was made based on the theory presented in the previous chapter and the simulations were made using the finite element method (FEM). Two types of harvesters were designed and simulated: one for industrial applications with resonant frequency in the 400-500Hz range and acceleration values over 1g (PZU1 energy harvester) and one for automotive applications with a resonant frequency below 100Hz and acceleration values below 0.5g (PZU2 energy harvester). The PZU2 design was possible directly on a desired resonant frequency of 86Hz due to the data provided by Renault Technologie Roumanie (RTR), a frequency chosen according to our technological capabilities.

Chapter 4 describes the process flow together with the masks set for each type of structure. The energy harvesters were also fabricated. Therefore, we obtained: 2

masks set (1 set of 5 masks for the PZU1 energy harvester and 1 set of 3 masks for the PZU2 energy harvester), PZU1 structures with 20 narrow cantilevers on a single chip and PZU2 structures with a single wide cantilever on a single chip, 1 fabrication technology of energy harvesters for industrial applications, 1 fabrication technology of energy harvesters for automotive applications and 1 technology for the thermal treatment of platinum layers depending on the desired application.

In *chapter 5* the previous-fabricated structures are tested.

For the **PZU1** harvester, only 10 out of 20 cantilevers could have been connected. These 10 were connected in 2 branches in series with 5 cantilevers connected in parallel on each branch. In laboratory conditions, an **electrical power of 2.53μW** was achieved at a **resonant frequency of 465.3Hz** and an **acceleration of 1g**. As a piezoelectric material, **Sc-doped (12%) AlN** was used, which is a lead-free material. At higher accelerations (2g), **a stabilized voltage of 1.8V** was achieved when the energy harvester was connected to the electronic module, based on the LTC3588-1 integrated circuit.

For the **PZU2** harvester, in laboratory conditions, an **electrical power of 2.28μW** was achieved at a **resonant frequency of 86Hz** and an **acceleration of 0.4g**. In this case, **PZT** was used as a piezoelectric material. At higher accelerations (2.5g), a **stabilized voltage of 2.5V** was obtained using the LTC3588-1 circuit. Testing in relevant conditions was also possible in this case, on a Dacia Jogger car at the Titu Technical Centre, RTR. The structures were tested for 3 scenarios and the results were similar with a commercial harvester, MIDE PPA 1021, from a power density point of view.

Chapter 6 contains the general conclusions from the theoretical and practical aspects of the research. Also, it summarizes the results, the original contributions and the prospects for further development.

The thesis ends with 3 annexes which present the less successful results of the research, but with great implications upon the learning process.

6.2 Original contributions

The results presented during this thesis are based on the original contributions of the author, confirmed through ISI-listed scientific publications, articles, papers presented at scientific conferences or patents. These are listed below; the paper in which it was presented is specified at every contribution, accordingly with the list from section 6.3.

1. *State-of-the-art synthesis regarding:*
   - The main types of piezoelectric energy harvesters for biomedical and environment applications [1]
   - Common materials used for fabrication of piezoelectric energy harvesters
   - Simulation/Modeling techniques using finite elements method (FEA)

2. *Masks set design for energy harvesters' fabrication:*
   - Piezoelectric energy harvester for industrial applications – silicon surface and bulk micromachining using 5 masks and SOI wafers [1, 9, 10, 11, 13]

- Piezoelectric energy harvester for automotive applications – silicon surface and bulk micromachining using 3 masks and SOI wafers

3. *Development of new technologies for the fabrication of piezoelectric energy harvesters* [1, 8, 9, 10, 11, 12, 13, 17]

4. *Studying and optimizing the DRIE etching process for structure release of cantilevers, with an effect in improving the MEMS process*

5. *Characterizing and testing of piezoelectric energy harvesters* [1, 8, 9, 10, 11, 12, 13]
    - Characterizing and testing in laboratory conditions for both harvesters, for industrial and automotive applications
    - Testing in relevant conditions (on Dacia Jogger car at Titu Technical Centre) of the energy harvester for automotive applications

In parallel to the activity of design, fabrication, characterization and testing of the energy harvesters, significant contributions were made for the fabrication technology of different types of sensors:
- piezoelectric sensors [10, 17]
- gas sensors [10, 3, 6, 7, 14, 15]
- pesticides/insecticides sensors [10, 4]
- biomedical sensors [10, 2, 5, 16]

The experience gained in developing the fabrication technology for these sensors was really useful in optimizing the process flow for the fabrication of the energy harvesters.

6.3 List of original publications

The research activity described in this thesis was possible thanks to **5 research projects** from IMT-Bucharest: PiezoMEMS *(2015-2018 M-era.Net, UEFISCDI contract no. 12/2015)*, PiezoHARV *(2017-2019 project STAR 2016, contract no. 164/2017)*, SENSIS 4 *(2018-2021 project COMPLEX PN-III-P1-1.2-PCCDI-2017-0419, contract no. 71 PCCDI/2018)*, SmartEnergy *(2021-2024 M-era.Net, UEFISCDI contract no. 240/2021)* and NET4Air *(2023-2025 HORIZON-WIDERA-2021-ACCESS-03, European Commission contract 101079455)*.

The original work is summarized in **7 articles published in ISI-listed journals** (1 article as main author (Q3) and co-author for 6 articles (2 Q1, 3 Q2 and 1 Q3)), **7 articles published in ISI-listed proceedings** (5 articles as main author and co-author for 2 articles), **co-author for 3 patents**, **8 papers presented at international conferences**, unpublished (5 as main author and 3 as co-author) and 5 scientific reports.

- **Articles published in ISI-listed journals**

1. **George Muscalu**, B. Firtat, A. Anghelescu, C. Moldovan, S. Dinulescu, C. Brasoveanu, M. Ekwinska, D. Szmigiel, M. Zaborowski, J. Zajac, A. Tulbure, *„Piezoelectric MEMS Energy Harvester for Low-Power Applications"*, Electronics 2024, 13(11), 2087; https://doi.org/10.3390/electronics13112087 - **AIS Quartile Q3**

2. R. C. Sandulovici, Mihailescu C.-M., A. Grigoroiu, C. A. Moldovan, M. Savin, V. Ordeanu, S. N. Voicu, D. Cord, G. M. Costache, M. L. Galatanu, M. Popescu, I. Sarbu, E. Mati, L. E. Ionescu, R. Neagu, V. Țucureanu, Rîmbu M. C., I. Mihalache, C. Romanitan, A. Piperea-Sianu, A. Boldeiu, O. Brincoveanu, C. E. Manea, B. Firtat, **George Stelian Muscalu**, D. Dragomir, *"The Physicochemical and Antimicrobial Properties of Silver/Gold Nanoparticles Obtained by "Green Synthesis" from Willow Bark and Their Formulations as Potential Innovative Pharmaceutical Substances"*, Pharmaceuticals 2023, 16(1), 48, https://doi.org/10.3390/ph16010048 - **AIS Quartile Q2**

3. A.Grigoroiu, C.-M. Mihailescu, M. Savin, C.A. Moldovan, C. Brasoveanu, S. Dinulescu, N. Djourelov, G.V. Cristian, O. Brincoveanu, G. Craciun, C. Pachiu, I. Stan, B. Firtat, **George Stelian Muscalu**, M. Ion, A. Anghelescu, *"Facile Electrodeposition-Based Chemosensors Using PANI and C-Hybrid Nanomaterials for the Selective Detection of Ammonia and Nitrogen Dioxide at Room Temperature"*, Chemosensors, vol. 11, no. 2, p. 132, Feb. 2023, https://doi.org/10.3390/chemosensors11020132 - **AIS Quartile Q2**

4. O. Tutunaru, C. M. Mihailescu, M. Savin, B. C. Tincu, M. C. Stoian, **George Stelian Muscalu**, B. Firtat, S. Dinulescu, G. Craciun, C. A. Moldovan, A. Ficai, A. C. Ion, *"Acetylcholinesterase entrapment onto carboxyl-modified single-walled carbon nanotubes and poly (3,4-ethylenedioxythiophene) nanocomposite, film electrosynthesis characterization, and sensor application for dichlorvos detection in apple juice"*, Microchemical Journal, Volume 169, October 2021, 106573, https://doi.org/10.1016/j.microc.2021.106573 - **AIS Quartile Q2**

5. C. M. Mihailescu, D. Stan, M. Savin, C. A. Moldovan, S. Dinulescu, C. H. Radulescu, B. Firtat, **George Muscalu**, C. Brasoveanu, M. Ion, D. Dragomir, D. Stan, A. C. Ion, *"Platform with biomimetic electrochemical sensors for adiponectin and leptin detection in human serum"*, Talanta Journal, Volume 210, Pages 120643, April 2020, https://doi.org/10.1016/j.talanta.2019.120643 - **AIS Quartile Q1**

6. B. Firtat, C. Moldovan, C. Brasoveanu, **George Muscalu**, M. Gartner, M. Zaharescu, P. Chesler, C. Hornoiu, S. Mihaiu, C. Vladut, I. Dascalu, V. Georgescu, I. Stan, *"Miniaturised MOX based sensors for pollutant and explosive gases detection"*, Sensors and Actuators B: Chemical Journal, Volume 249, Pages 647-655, October 2017, https://doi.org/10.1016/j.snb.2017.04.032 - **AIS Quartile Q1**

7. P.Chesler, C. Hornoiu, S. Mihaiu, C. Vladut, J.M. Calderon Moreno, M. Anastasescu, C. Moldovan, B. Firtat, C.Brasoveanu, **George Muscalu**, I. Stan

and M. Gartner, *"Nanostructured SnO2-ZnO composite gas sensors for selective detection of CO"*, Beilstein Journal of Nanotechnology, 7, 2016, 2045-2056, https://doi.org/10.3762/bjnano.7.195 - **AIS Quartile Q3**

- **Articles published in ISI-listed proceedings**

8. **George-Stelian Muscalu**, N. Varachiu, B. Firtat, S. Dinulescu, A. Tulbure, C. Moldovan, *"Vibrational energy harvesting devices for Structural Health Monitoring–Design optimization"*, 2020 International Semiconductor Conference (CAS), Sinaia, Romania, 2020, pp. 151-154, https://doi.org/10.1109/CAS50358.2020.9268030

9. M. A Ekwińska, J. Zając, D. Szmigiel, M. Zaborowski, C. Jastrzębski, **George Muscalu**, B. Firtat, S. Dinulescu, A. Anghelescu, C. Moldovan, *"Advantages of Using Piezoelectric Materials in the MEMS Construction on the Example of AlN and Sc Doped AlN Layers"*, Mechatronics 2019: Recent Advances Towards Industry 4.0. MECHATRONICS 2019. Advances in Intelligent Systems and Computing, vol 1044. Springer, Cham, September 2019, https://doi.org/10.1007/978-3-030-29993-4_33

10. **George Muscalu**, C. Romanitan, B. Bita, S. Dinulescu, A. Anghelescu, C. Moldovan, *"Effect of temperature treatments in different atmospheres on the crystallographic orientation and sheet resistance of Pt/Ti films on silicon"*, 2017 International Semiconductor Conference (CAS), Sinaia, Romania, 2017, pp. 279-282, https://doi.org/10.1109/SMICND.2017.8101224

11. **George Muscalu**, B. Firtat, S. Dinulescu, C. Moldovan, A. Anghelescu, I. Stan, *"Power Harvesting and Storage Circuit for a Double Array of Lead-Free Piezoelectric Cantilevers"*, 2018 International Semiconductor Conference (CAS), Sinaia, Romania, 2018, pp. 321-324, https://doi.org/10.1109/SMICND.2018.8539803

12. **George Muscalu**, B. Firtat, S. Dinulescu, C. Moldovan, A. Anghelescu, C. Vasile, D. Ciobotaru, C. Hutanu, *"Design and Simulation of Piezoelectric Energy Harvester for Aerospace Applications"*, 2018 International Semiconductor Conference (CAS), Sinaia, Romania, 2018, pp. 325-328, https://doi.org/10.1109/SMICND.2018.8539767

13. **George Muscalu**, A. Anghelescu, B. Firtat, *"Design optimization of MEMS piezoelectric energy cantilever device for environment vibrations harvesting"*, 2015 International Semiconductor Conference (CAS), Sinaia, Romania, 2015, pp. 267-270, https://doi.org/10.1109/SMICND.2015.7355228

14. A. Grigoroiu, C.-M. Mihailescu, M. Savin, C. Brașoveanu, C.-A. Moldovan, S. Dinulescu, **George-Stelian Muscalu**, O. Brincoveanu, B. Firtat, M. Ion, D. Dragomir, Adrian Anghelescu, *"Enhancing NO2 gas sensing performance at room temperature using electrodeposited composite Ppy-rGO-Fc"*, 2023 International Semiconductor Conference (CAS), Sinaia, Romania, 2023, pp. 43-46, https://doi.org/10.1109/CAS59036.2023.10303719

- **Patents**

15. C.A. Moldovan, C.M.Mihăilescu, M. Savin, B. Fîrtat, A. Grigoroiu, C. Brașoveanu, S. Dinulescu, **George Stelian Muscalu**, V.C. Georgescu, I. Stan, *"Procedeu de realizare film compozit sensibil la amoniac bazat pe electrodepunerea materialului compozit PANI/MWCNT-NH2/PSS"*, RO-BOPI 01/2024, G01N 30/64, https://osim.ro/images/Publicatii/Inventii/2024/bopi_inv_01_2024.pdf

16. C.M. Mihăilescu, M. Savin, C.A. Moldovan, B. Firtat, **George Stelian Muscalu**, M. Ion, F.A Boldeiu, C. Romanițan, O.A. Brincoveanu, I. Mihalache, *"Procedeu de sinteză și caracterizare molecule de detecție folosite pentru dezvoltarea de teste rapide imunocromatografic"*, RO-BOPI 11/2023, G01N 33/53, https://osim.ro/images/Publicatii/Inventii/2023/inv_11_2023.pdf

17. G. Marin, C. Moldovan, M. Gartner, **George Muscalu**, H. Stroescu, C. Brasoveanu, *"Procedeu de obținere a soluției de precursori pentru depunerea prin metoda sol-gel a straturilor de PZT"*, RO-BOPI 06/2021, C23C18/48, RO a201800598, https://osim.ro/wp-content/uploads/Publicatii-OSIM/BOPI-Inventii/2021/bopi_inv_02_2021.pdf

- **Presentations at international conferences**

18. **George Muscalu**, S. Dinulescu, C. Moldovan, B. Firtat, A. Anghelescu, G. Sirbu, N. Boicea, J. Zając, M. Ekwińska, D. Szmigiel, *"Piezoelectric MEMS energy harvester for automotive applications"*, EpoSS Annual Forum 2024, 18–21 iunie 2024, Cork, Ireland – nepublicat in volum

19. J. Zając, M. Ekwinska, Helena Klos, D. Szmigiel, **George Muscalu**, S. Dinulescu, C. Moldovan, B. Firtat, A. Anghelescu, G. Sirbu, N. Boicea, *"Maintenance-free energy source made of SOI wafers and piezoelectric materials: AlN:Sc and PZT"*, 10th Joint International EuroSOI Workshop and International Conference on Ultimate Integration on Silicon (EuroSOI-ULIS) 2024, 15-17 mai 2024, Atena, Grecia – nepublicat in volum

20. **George Muscalu**, S. Dinulescu, B. Firtat, A. Anghelescu, C. Moldovan, C. Brasoveanu, A. Tulbure, M. Ekwińska, D. Szmigiel, M. Zaborowski, J. Zając, G. Sirbu, N. Boicea, *„Piezoelectric MEMS energy harvester for ultra-low power applications"*, 2023 International Semiconductor Conference (CAS), Sinaia, Romania, 2023 – nepublicat in volum

21. D. Belavic, K. Vojisavljevic, D. Kuscer, T. Pecnik, J. Zajac, A. Anghelescu, **George Muscalu**, M. Hodnik, T. Kos, S. Drnovsek, B. Malic, *"Ceramic packaging of PiezoMEMS devices"*, 2017 21st European Microelectronics and Packaging Conference (EMPC) & Exhibition, Warsaw, Poland, 2017, pp. 1-4, https://doi.org/10.23919/EMPC.2017.8346888

22. **George Muscalu**, B. Firtat, S. Dinulescu, A. Anghelescu, C. Moldovan, M. Ekwińska, D. Szmigiel, M. Zaborowski, J. Zając, *"Piezoelectric energy harvester for wireless sensor networks"*, 2019 ISAF-ICE-FEM-IWPM-PFM Joint Conference – f2cπ2, 14-19 iulie 2019, Lausanne, Elveția – nepublicat in volum

23. **George Muscalu**, B. Fîrtat, S. Dinulescu, A. Anghelescu, C. Moldovan, M. Gartner, M. Zaharescu, M. Anastasescu, H. Stroescu, S. Mihaiu, M. Ekwińska, D. Szmigiel, M. Zaborowski, J. Zając, *"Piezoelectric energy harvester for environmental applications"*, EuroNanoForum 2019, 12-14 iunie 2019, Bucharest, Romania – nepublicat in volum

24. **George Muscalu**, B. Fîrtat, S. Dinulescu, C. Moldovan, A. Anghelescu, D. Varsescu, A. Avram, S. Vulpe, *"Fabrication and mechanical testing of MEMS piezoelectric cantilevers array for energy harvesting"*, Micro and Nano Engineering Conference (MNE), 24-27 Septembrie 2018, Copenhagen, Denmark – nepublicat in volum

25. B. Fîrtat, C. Moldovan, A. Anghelescu, **George Muscalu**, P. Schiopu, *„Lead-free piezoelectric MEMS cantilever for energy harvesting – design, optimization and technology"*, Smart Systems Integration 2017 Conference, 8-9 Martie 2017, Cork, Ireland – nepublicat in volum

- **Scientific reports**

26. Scientific report no. 1, *Microsisteme piezoelectrice de captare a energiei pentru aplicații biomedicale și de mediu – considerații teoretice și rezultate preliminarii*;

27. Scientific report no. 2, *Optimizarea proceselor tehnologice esențiale în obținerea unui microsistem de captare a energiei pentru aplicații de mediu*;

28. Scientific report no. 3, *Obtinerea unui microsistem de captare a energiei pentru aplicații de mediu și optimizarea proceselor tehnologice*;

29. Scientific report no. 4, *Dezvoltarea modulului electronic de stocare și livrare controlată a energiei*;

30. Scientific report no. 5, *Integrarea dispozitivului MEMS, a straturilor piezoelectrice și a modulului electronic*;

6.4 Perspectives for further developments

These types of microsystems are focused on ultra-low-power applications (1-100μW). Even though we reached this power range with our fabricated energy harvesters, these were achieved mainly in laboratory conditions. This proved the potential of the piezoelectric energy harvesters for energy supplying of microsensors or microsystems.

A first step in further developments is the publishing of the newest results for the PZU2 energy harvester. The next step is optimizing the structures in order to harvest energy from a larger bandwidth.

Another step is gaining the capability of fabrication of piezoelectric layers at IMT-Bucharest. Validating this step allows us a much faster approach in harvester's fabrication. Also, using suitable encapsulation (in vacuum) it is possible to reach a better TRL level (*Technology Readiness Level*).

In the future, optimization of other technological processes could be also improved due to the experience gained during the doctoral studies.

Annexes

A1 Process flow for test structures of piezoelectric layers

Test structures were designed and fabricated in order to characterize the piezoelectric layers with the end scope of integrating them with the available MEMS technologies. These are easier to employ and have a lower cost of implementation.

The test structures consist in cantilever structures with a thickness as same as the wafer thickness. The measurement principle is based in the reverse piezoelectric effect.

A2 Piezoelectric energy harvester for aerospace applications – PZU3

PZU3 energy harvester was designed to harvest energy from the vibrations on a tail plane of a PZL SW-4 helicopter. These vibrations are at 30, 45 and 90Hz with accelerations of 15.4, 8.6 and 1.5 m/s^2.

PZT was chosen as a piezoelectric material and it was deposited by spinning. Even though this process couldn't have been integrated with the available MEMS technologies, the deposition method was improved resulting in a patent [14]. The fabricated structures are presented in **Fig. A2.12** and **Fig. A2.17**, without a functional piezoelectric material.

Fig. A2.12. Initial PZU3 structures   *Fig. A2.17. Fabricated spiral PZU3 structures*

A3 Piezoelectric energy harvester for civil infrastructure applications – PZU4

The PZU4 energy harvester (**Fig. A3.5**) was designed to harvest energy from the vibrations of a wooden bridge attended by people. The vibration frequency is around 385Hz. 5 cantilevers groups were fixed together with a common proof mass in order to avoid phase differences and AlN was used as a piezoelectric material. The maximum generated power was way below expectations, of 0.046μW, due to the mechanical failure of the cantilevers (**Fig. A3.12**).
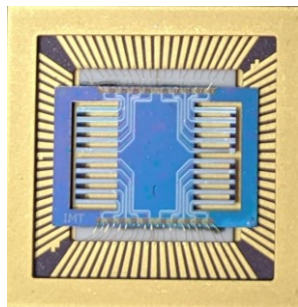
Fig. A3.5. PZU4 energy harvester   *Fig. A3.12. Mechanical failure of cantilvers*
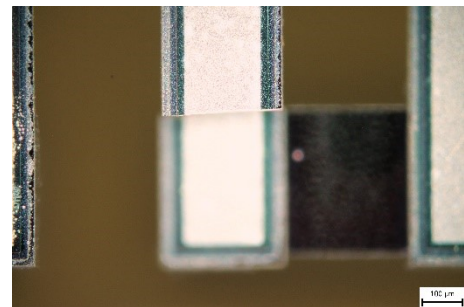
Bibliography – selection

[1]   M. Yip, "Ultra-low-power circuits and systems for wearable and implantable medical devices," Thesis, Massachusetts Institute of Technology, 2013. Accessed: Jun. 09, 2024. [Online]. Available: https://dspace.mit.edu/handle/1721.1/84902

[2]   "Energy Harvesting System Market Size, Share, Industry Trends Forecast, Opportunities 2030," MarketsandMarkets. Accessed: Mar. 26, 2024. [Online]. Available: https://www.marketsandmarkets.com/Market-Reports/energy-harvesting-market-734.html

[3]   N. Jackson, R. O'Keeffe, F. Waldron, M. O'Neill, and A. Mathewson, "Evaluation of low-acceleration MEMS piezoelectric energy harvesting devices," *Microsyst Technol*, vol. 20, no. 4, pp. 671–680, Apr. 2014, doi: 10.1007/s00542-013-2006-6.

[4]   Y. Jia and A. A. Seshia, "Power Optimization by Mass Tuning for MEMS Piezoelectric Cantilever Vibration Energy Harvesting," *J. Microelectromech. Syst.*, vol. 25, no. 1, pp. 108–117, Feb. 2016, doi: 10.1109/JMEMS.2015.2496346.

[5]   C. B. Williams and R. B. Yates, "Analysis of a micro-electric generator for microsystems," *Sensors and Actuators A: Physical*, vol. 52, no. 1–3, pp. 8–11, Mar. 1996, doi: 10.1016/0924-4247(96)80118-X.

[6]   G. Muscalu, A. Anghelescu, and B. Firtat, "Design optimization of MEMS piezoelectric energy cantilever device for environment vibrations harvesting," in *2015 International Semiconductor Conference (CAS)*, Oct. 2015, pp. 267–270. doi: 10.1109/SMICND.2015.7355228.

[7]   G. Muscalu, C. Romanitan, B. Bita, S. Dinulescu, A. Anghelescu, and C. Moldovan, "Effect of temperature treatments in different atmospheres on the crystallographic orientation and sheet resistance of Pt/Ti films on silicon," in *2017 International Semiconductor Conference (CAS)*, Oct. 2017, pp. 279–282. doi: 10.1109/SMICND.2017.8101224.

[8]   G. Muscalu *et al.*, "Piezoelectric MEMS Energy Harvester for Low-Power Applications," *Electronics*, vol. 13, no. 11, p. 2087, May 2024, doi: 10.3390/electronics13112087.

[9]   G. Muscalu, B. Firtat, S. Dinulescu, C. Moldovan, A. Anghelescu, and I. Stan, "Power Harvesting and Storage Circuit for a Double Array of Lead-Free Piezoelectric Cantilevers," in *2018 International Semiconductor Conference (CAS)*, Sinaia: IEEE, Oct. 2018, pp. 321–324. doi: 10.1109/SMICND.2018.8539803.

[10] G. Muscalu *et al.*, "Piezoelectric MEMS energy harvester for automotive applications," presented at the EpoSS Annual Forum 2024, Cork, Irlanda, 21 iunie 2024.

[11] Y. Liu *et al.*, "Design and Performance of ScAlN/AlN Trapezoidal Cantilever-Based MEMS Piezoelectric Energy Harvesters," *IEEE Transactions on Electron Devices*, vol. 68, no. 6, pp. 2971–2976, Jun. 2021, doi: 10.1109/TED.2021.3072612.

[12] X. He, D. Li, H. Zhou, X. Hui, and X. Mu, "Theoretical and Experimental Studies on MEMS Variable Cross-Section Cantilever Beam Based Piezoelectric Vibration Energy Harvester," *Micromachines*, vol. 12, no. 7, p. 772, Jun. 2021, doi: 10.3390/mi12070772.

[13] X. Zhao, Z. Shang, G. Luo, and L. Deng, "A vibration energy harvester using AlN piezoelectric cantilever array," *Microelectronic Engineering*, vol. 142, pp. 47–51, Jul. 2015, doi: 10.1016/j.mee.2015.07.006.

[14] G. Marin, C. Moldovan, M. Gartner, G. Muscalu, H. Stroescu, and C. Brasoveanu, "Procedeu de obţinere a soluţiei de precursori pentru depunerea prin metoda sol-gel a straturilor de PZT," RO-BOPI 06/2021, C23C18/48, RO a201800598 [Online]. Available: https://osim.ro/wp-content/uploads/Publicatii-OSIM/BOPI-Inventii/2021/bopi_inv_02_2021.pdf